ACS OMEGA

Open Access



http://pubs.acs.org/journal/acsodf

Article

# Synthesis of a Cannabidiol Precursor: Experimental Challenges and DFT Insights into β-Elimination Barriers

Michael Bergami, Claudio Trapella, Greta Compagnin, Simona Felletti, Martina Catani, Silvia Pezzola, Federica Sabuzi, Pierluca Galloni, Paolo Marchetti, Virginia Cristofori, Anna Fantinati,* and Davide Illuminati

Cite This: *ACS Omega* 2026, 11, 5413−5420

Read Online

ACCESS | Metrics & More | Article Recommendations | Supporting Information

**ABSTRACT:** The synthesis of cannabidiol (CBD) from limonene derivatives involves a key β-elimination step that remains challenging to reproduce efficiently. In this work, we revisited a known racemic synthetic route to CBD and investigated the mechanistic origin of the low yield associated with the β-hydrogen elimination step. Alternative synthetic approaches were tested experimentally by comparing the traditional selenoxide-mediated pathway with a direct elimination attempt from bromohydrin intermediates. Despite optimization of reaction and workup conditions, β-elimination consistently failed, regenerating epoxide **1** instead of olefin **3**. Density functional theory (DFT) calculations revealed that conformational constraints and electronic effects disfavor the reactive rotamer required for β-hydrogen elimination, explaining the experimentally observed lack of reactivity. The results clarify why the selenoxide pathway remains the only viable route to p-mentha-2,8-dien-1-ol (**3**) and provide mechanistic insight that may guide the development of future selenium-free synthetic methods.

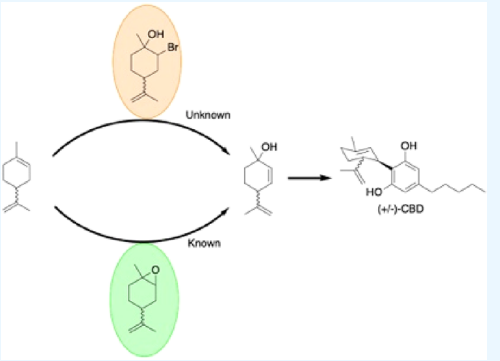


## INTRODUCTION

*Cannabis sativa L.* has been used by humans for centuries for both medicinal and industrial purposes.[1] In recent years, its bioactive constituents—cannabinoids—have attracted increasing scientific attention for their therapeutic potential. The main cannabinoids, $\Delta^9$-tetrahydrocannabinol (THC) and cannabidiol (CBD), are responsible for the psychoactive and therapeutic effects of the plant, respectively.[2,3] These molecules interact with the endocannabinoid system, influencing processes such as pain perception, inflammation, and mood regulation. Recent medicinal chemistry studies continue to highlight the therapeutic relevance of cannabinoids in neuropathic pain.[4] The stereochemical configuration of these compounds critically affects their pharmacological profile, as exemplified by the distinct biological activities of (−)-CBD and its (+)-enantiomer.[5−7]

Beyond their biological relevance, cannabinoids are also of great synthetic and mechanistic interest. Over the past decades, numerous synthetic approaches to CBD and related analogues have been reported, differing mainly in how the terpenoid and resorcinol fragments are assembled. Among them, the Friedel−Crafts alkylation between olivetol and a terpene-derived allylic alcohol represents one of the most concise and widely employed methods.[8] This reaction, typically catalyzed by Lewis acids such as $BF_3{\cdot}Et_2O$, establishes the key C−C bond connecting the aromatic and terpenoid portions of the molecule.

In this context, p-mentha-2,8-dien-1-ol (**3**) is a pivotal intermediate for the synthesis of both enantiomers of CBD. Efficient access to this compound from limonene or related monoterpenes is therefore essential for the development of versatile synthetic routes toward cannabinoids. The present work focuses on optimizing the synthesis of compound **3** through selenium-mediated and alternative bromohydrin pathways, supported by DFT calculations that provide mechanistic insights into the β-elimination step.

For clarity, Scheme 1 first illustrates the general Friedel−Crafts alkylation leading from intermediate **3** and olivetol (**4**)

**Scheme 1. Coupling between (3) and Olivetol (4) to Obtain (±)-CBD**

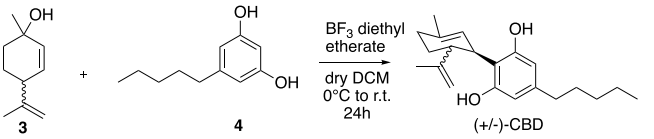


Received: August 25, 2025
Revised: December 3, 2025
Accepted: December 5, 2025
Published: January 21, 2026

to racemic CBD ((±)-CBD), followed by Scheme 2 (in the Results and Discussion section), which details the synthetic

**Scheme 2. Classical Synthesis to Obtain P-Mentha-2,8-dien-1-ol (3)**

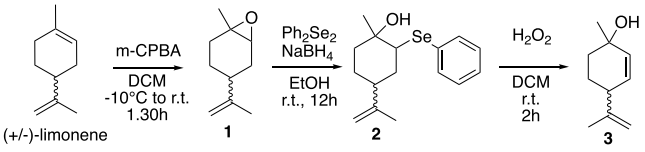


routes investigated to obtain compound **3**. This sequence highlights the central role of intermediate **3** in CBD synthesis and motivates the computational analysis presented later.

The aim of our study was to evaluate various synthetic strategies to access p-mentha-2,8-dien-1-ol (**3**), a key intermediate in the synthesis of (±)-CBD. Despite the predominance of stereoselective syntheses for (−)-CBD in the literature, we opted for a racemic approach (Scheme 2) to obtain the racemic mixture and testing the analytical methodologies able to separate the enantiomers that could be applied to the identification of other cannabinoids from the natural source.

## RESULTS AND DISCUSSION

As reported in the literature,[9] our synthesis commenced with commercially available (±)-limonene, which was converted into cis/trans limonene epoxide (**1**). This epoxide was subsequently opened by using a selenium reagent, followed by an elimination reaction. Upon obtaining p-mentha-2,8-dien-1-ol (**3**), the final step involved a coupling reaction with olivetol (**4**) using a Lewis acid, such as boron trifluoride etherate[9] (Scheme 1).

To verify the stereochemical outcome of our synthetic route, the final product was analyzed by chiral HPLC. As expected, given that the synthesis started from racemic (±)-limonene and no chiral reagents or catalysts were employed, the resulting cannabidiol was racemic (ee ≈ 0.1%). The chiral HPLC analysis confirmed the presence of both (+)-CBD and (−)-CBD, demonstrating the effectiveness of the chromatographic method for resolving CBD enantiomers. Although in this work the separation was demonstrated only for cannabidiol, this approach could potentially be extended to the enantiomeric analysis and resolution of other cannabinoids in future studies (Figures S2−S5, Supporting Information).

The major problems encountered by this process were:

1- the minimal formation of the double epoxidation product;
2- the formation of the tertiary rather than secondary selenide derivative and therefore the consequent exo elimination product (Scheme 3).

The synthetic step involving the formation of the selenide intermediate is facilitated by using diphenyl diselenide in conjunction with a reducing agent, sodium borohydride. The formation of a tertiary selenide byproduct is attributed to the acidic nature of the solvent ethanol (EtOH). To optimize the yield, we explored various solvent mixtures, such as tetrahydrofuran: THF/EtOH and THF/MeOH. While these mixtures successfully suppressed the formation of compound **6**, the reactions remained incomplete due to the presence of

**Scheme 3. Byproducts of This Route**

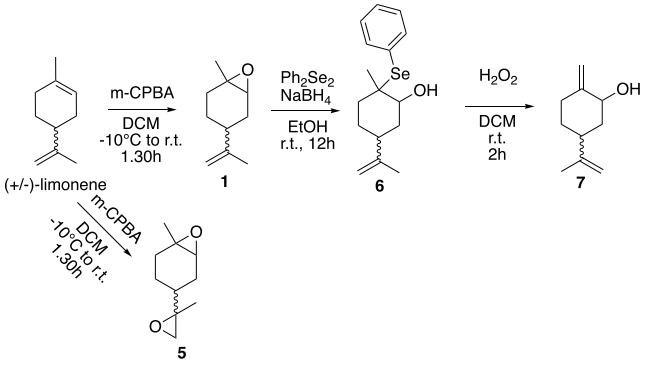


unreacted starting material (see Table S4 in the Supporting Information).

To address these challenges, an alternative strategy was devised. The epoxidation step was replaced with the formation of bromohydrin (**8**) using N-bromosuccinimide (NBS), followed by a conventional substitution reaction.

When comparing the two approaches for forming the selenide intermediate **2**, the route proceeding through the epoxide afforded an overall yield of 16%, whereas the pathway involving the bromohydrin **8** provided a significantly higher overall yield of 44%. This result clearly demonstrates the greater efficiency of the bromohydrin-based route, likely due to the milder reaction conditions and higher stability of compound **8** relative to that of epoxide **1**.

The formation of bromohydrin **8** and epoxide **1** from limonene provided comparable yields (50% and 60%, respectively). However, a marked difference was observed in the subsequent substitution step (Scheme 4): conversion of bromohydrin **8** into selenide **2** using diphenyl diselenide and $NaBH_4$ afforded an 85% yield, whereas the analogous transformation from epoxide **1** proceeded with a significantly lower yield. As a result, the overall yield of compound **2** through the bromohydrin route was considerably higher than that obtained via the epoxide pathway. Finally, oxidation of the selenide intermediate with hydrogen peroxide, in the absence of pyridine as reported by Mori,[9] efficiently generated the corresponding selenoxide, which underwent syn $\beta$-elimination via selenoxide, where the carbon−hydrogen and carbon−selenium bonds are coplanar in the transition state, as illustrated in Figure 1.[10]

The low yield observed in the final step (which leads to **3**) prompted us to consider a more direct synthetic alternative. To develop a selenium-free route to compound **3**, we investigated the possibility of accessing it directly from bromohydrin **8** through a base-promoted $\beta$-elimination (E2) mechanism. This approach bypasses the formation and oxidation of the selenide intermediate, offering a potentially simpler and more sustainable pathway.

However, when various bases were tested (see Table S4 in the Supporting Information), the competing intramolecular substitution dominated, leading to the reformation of epoxide **1** instead of the desired olefin **3**. The failure of this transformation provides valuable mechanistic insight into why such a seemingly straightforward E2 route is not typically employed in cannabinoid synthesis. The results are summarized in Scheme 4, where an additional arrow highlights the hypothetical direct conversion from 8 to 3, underscoring both


https://doi.org/10.1021/acsomega.5c08636
ACS Omega 2026, 11, 5413−5420

**Scheme 4. Bromohydrin Formation Pathway**

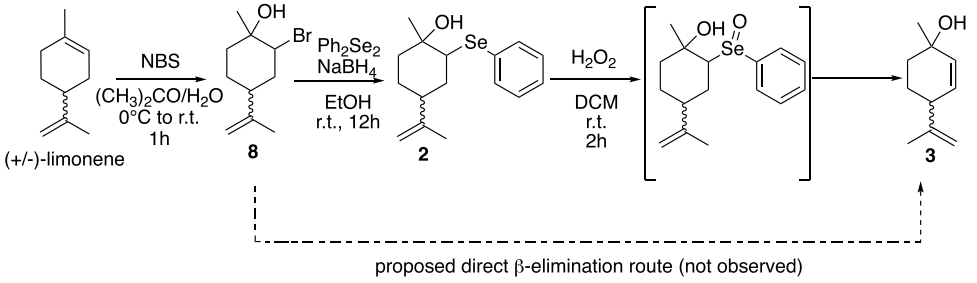


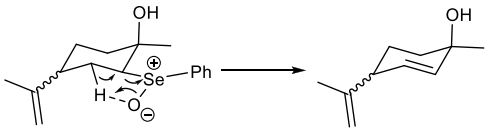


**Figure 1.** Elimination by selenoxide.

the conceptual appeal and the current limitations of this strategy.

When bromohydrin **8** was treated with a base, instead of undergoing *β*-elimination, it underwent intramolecular substitution to regenerate epoxide **1** (Scheme 5). This outcome demonstrates that under these conditions, the leaving group departs via an SN2 mechanism rather than an E2 pathway. To suppress this competing cyclization and favor elimination, we next examined protected derivatives of **8**, namely, acetate **9** and alkoxide **10**. However, in both cases, the desired formation of olefin **3** was not observed.

To better understand the reasons why the reaction did not proceed as expected, a detailed DFT study was conducted. For the sake of simplicity, calculations were performed considering only one limonene enantiomer, i.e., (+)-limonene.

Calculations were performed using the range-separated hybrid (RSH)-GGAs functional WB97XD[11] that well describes positively charged molecules and/or cations.[12] Solvation model based on density (SMD) was selected for its capability in mimicking the charge density of the medium,[13,14] while 6−311 G+(d,p) was selected as basis set for its ability to well describe small organic compounds with an acceptable computational cost.[15,16]

First, the relative stability of the carbocation intermediates formed upon "$Br^{+}$" addition to (+)-limonene, namely, *syn* or *anti* intermediates, with respect to the isopropenyl group was investigated, mimicking the experimental conditions of the reaction between limonene and NBS (i.e., acetone as the solvent, at 298.15 K). Gibbs energies (G) of the optimized intermediates are reported in Table S1 (see the Supporting Information).

Optimized geometries are reported in Figure 2. Results showed that the most stable intermediate is the one obtained

**Scheme 5. Elimination from (Protected) Bromohydrin Does Not Occur**[a]

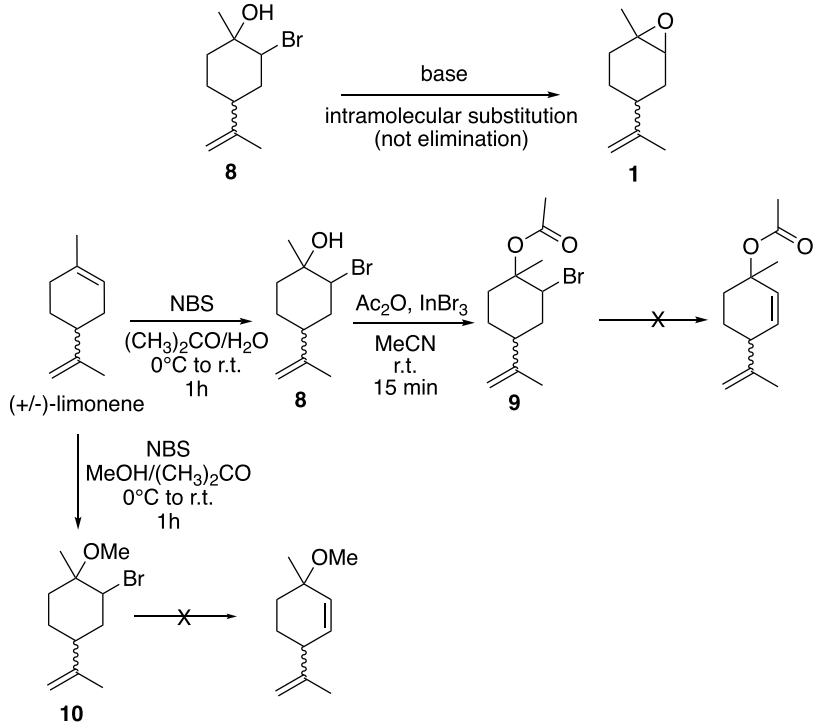


[a]Treatment of bromohydrin **8** with base leads to epoxide **1** via intramolecular substitution, while elimination attempts from acetate **9** or alkoxide **10** also fail to yield olefin **3**



https://doi.org/10.1021/acsomega.5c08636
ACS Omega 2026, 11, 5413−5420

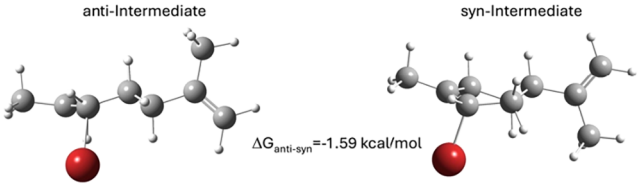


**Figure 2.** Geometry optimization of *syn*- and *anti*- intermediates obtained with WB97XD/SMD/6−311 G+(d,p).

with "$Br^+$" addition in *anti* with respect to the isopropenyl group, likely due to the lower steric hindrance of the bulky substituent ($\Delta G_{anti\text{-}syn}$ = −1.59 kcal/mol).

Afterward, conformational equilibria of the possible diastereomers of product **10**, obtained from the following insertion of $-OCH_3$ group at the carbocation intermediates, were studied. Thus, the relative stabilities of diastereomers **A** and **B** (Figure 3) were analyzed. Specifically, diastereomer **A**

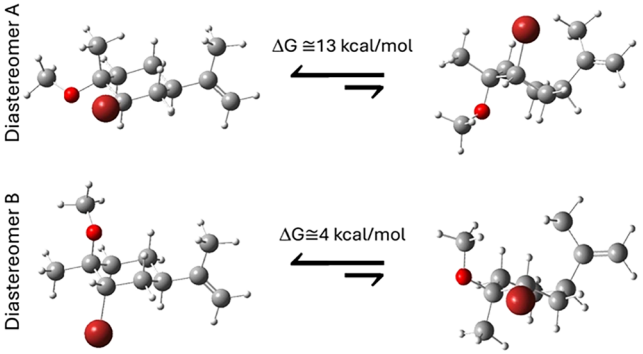


**Figure 3.** Geometries of conformers **A** and **B** with WB97XD/SMD/6−311G+(d,p). DG: Gibbs energy difference between conformations of the left and right columns.

originates from the attack of the double bond of (+)-limonene to "$Br^+$" in *syn* with respect to the isopropenyl group; then, methoxy group addition occurs in *anti* with respect to Br. Conversely, diastereomer **B** originates from the nucleophilic attack of the double bond to "$Br^+$" in *anti* with respect to the isopropenyl group. Chair conformations of diastereomers **A** and **B** were analyzed and compared, to find out the most stable one (Figure 3). In this scenario, according to experimental conditions for elimination reaction, geometry optimizations and energy calculations were performed in THF, at 203 and 273 K.

Concerning diastereomer **A**, the most stable conformer has the bulky groups (i.e., -Br, -OMe, -isopropenyl) in equatorial position. Indeed, it is ca. 13 kcal/mol more stable than the corresponding conformer with the same groups in axial position. As for the diastereomer **B**, the most stable conformer was achieved with -Br and -OMe in axial position ($\Delta G \sim 4$ kcal/mol, Table S2, see the Supporting Information). In addition, under these experimental conditions, *in silico* outputs at both temperatures suggest that diastereomer **B** is more stable than **A** ($\Delta G_{B\text{-}A}$ = −0.35 kcal/mol at 203 K, and −0.50 kcal/mol at 273 K). Furthermore, considering the higher stability of the carbocation intermediate obtained upon the addition of "$Br^+$" in *anti* to the isopropenyl group, with respect to the *syn* intermediate ($\Delta G_{anti\text{-}syn}$ = −1.59 kcal/mol, Figure 2), formation of **B** is favored over **A**.

Nevertheless, such findings do not explain why *β*-elimination from **10** did not occur. As a matter of fact, considering the most stable conformer, diastereomer **B** could undergo elimination because of the presence of -Br in the axial position. Thus, an in-depth potential map analysis of diastereomer **B** in the most stable chair conformation was performed (Figure 4a-a').

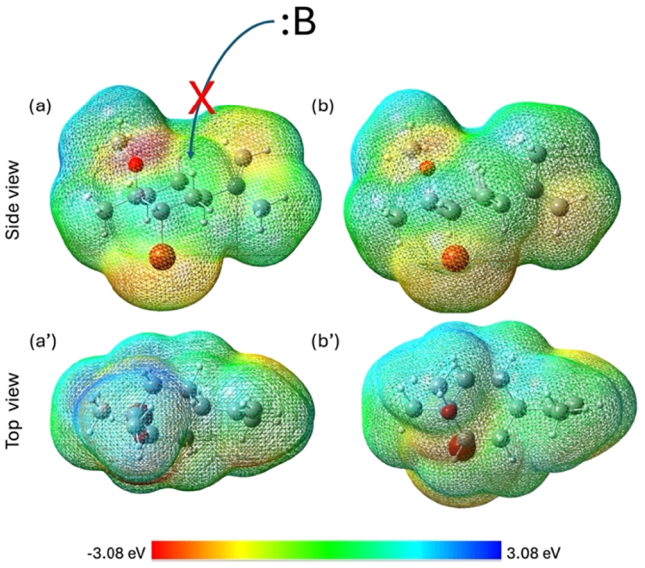


**Figure 4.** Potential map analysis of two possible rotamers of **B** around bond $C_4-C_{1'\text{-isopropenyl}}$. (a, a') Double bond of the isopropenyl group directed above the plane that includes the ring. (b, b') Double bond of the isopropenyl group directed below the plane that includes the ring. Geometry was optimized with a WB97XD/SMD/6−311G+(d,p) at 203 K.

Results show that a high electron density extends from the methoxy group to the double bond of the isopropenyl group. Such extended electron density likely shields the approach of a base (even if not bulky, such as a hydride) due to electrostatic repulsion. Therefore, in the most stable conformation of diastereomer **B**, the axial proton in *β*-position with respect to -Br is actually unavailable for elimination.

Importantly, the rotation of $C_4-C_{1'\text{-isopropenyl}}$ was also considered. In particular, a detailed analysis of the energy profile associated with the possible rotations of the isopropenyl group was performed for both conformers of diastereomer **B** (Figure S1, see the Supporting Information). Indeed, considering the 180° rotation of $C_4-C_{1'\text{-isopropenyl}}$ (Figure 4b-b'), the electron density would be localized on the methoxy group, likely allowing *β*-elimination. However, the calculated Gibbs energy demonstrated that the most stable rotamer in the adopted reaction conditions, namely, in THF as solvent at 203 or 273 K, is the one described in panels a-a'. In particular, an energy difference between the two rotamers was detected ($\Delta G_{203\ K}$ = −0.30 kcal/mol; $\Delta G_{273\ K}$ = −0.45 kcal/mol), suggesting that, in the experimental conditions, the most populated rotamer is the nonreactive one (Table S3, see the Supporting Information).

To sum up, computational analysis suggested that in the adopted reaction conditions, even if the formation of diastereomer **B** is favored over **A** from an energetic point of view, the following *β*-elimination is prevented by electrostatic effects, which hampers the approach of a base to the *β*-proton.



https://doi.org/10.1021/acsomega.5c08636
ACS Omega 2026, 11, 5413−5420

## CONCLUSIONS

In this work, we investigated alternative synthetic routes to p-mentha-2,8-dien-1-ol (**3**), which is a key intermediate in the synthesis of cannabidiol (CBD). Two pathways for the formation of selenide intermediate **2** were compared: one proceeding through epoxide **1** and the other through bromohydrin **8**. The bromohydrin-based route afforded a markedly higher overall yield compared to the epoxide pathway, demonstrating its synthetic advantage under milder conditions.

To further simplify the synthesis, a direct selenium-free approach was evaluated via $\beta$-hydrogen elimination (E2) from bromohydrin **8**. However, this transformation did not occur as the competing intramolecular substitution leading to epoxide **1** dominated under all tested conditions. Thus, the $\beta$-elimination issue remains experimentally unresolved; nevertheless, the combined experimental and computational results provide a clear mechanistic understanding of this limitation. DFT calculations confirmed that $\beta$-hydrogen elimination is thermodynamically and kinetically disfavored because the most stable rotamer of the **8** is nonreactive within the studied temperature range.

Overall, the present results clarify why the seemingly straightforward E2 route to compound **3** has not been reported in the literature and emphasize the role of the selenoxide pathway as the most reliable strategy for $\beta$-elimination in this system. These findings provide a mechanistic basis for the future development of more sustainable selenium-free methods for accessing cannabinoid intermediates.

## EXPERIMENTAL SECTION

### General Experimental Procedures

Unless otherwise stated, reagents and solvents were purchased from Sigma-Aldrich (Milan, Italy), Fluorochem (Hadfield, United Kingdom), or TCI (Zwijndrecht, Belgium) and used without further purification. All reactions were monitored by TLC on silica gel (Merck precoated 60F254 plates) with detection by UV light (254 nm) or by potassium permanganate. Analytical separations have been performed on an AZURA HPLC system (KNAUER, Berlin, Germany) equipped with a binary high-pressure gradient pump (max pressure: 862 bar), a column thermostat, an autosampler, and a photodiode array detector. A 250 mm × 4.6 mm Chiralpak IG column packed with 5 $\mu$m particles was kindly supplied by Chiral Technologies Europe (Illkirch, France). The isocratic elution method was acetonitrile−water (60−40%). The flow rate was 1 mL/min, the column temperature was set at 25 °C, and the detection wavelength was 228 nm. Standard solution (1 mg/mL) of cannabinoid (−)-CBD was purchased from Cerilliant (Round Rock, TX, USA). Products were purified by flash column chromatography using silica gel Merck 60 (230−400 mesh) as the stationary phase or by Isolera One, Biotage. $^1$H NMR spectra were recorded on a Bruker Avance Spectrometer 500 MHz or on a VARIAN 400 MHz, and $^{13}$C NMR spectra were recorded on the same instrument 126 MHz (for Bruker) or 101 MHz (for VARIAN), using commercially available deuterated (chloroform-d) solvent at room temperature. Chemical shifts are reported in parts per million (ppm). Multiplicities in $^1$H NMR are reported as follows: s−singlet, d−doublet, t−triplet, m−multiplet, br−broad. Data for $^{13}$C NMR are reported in chemical shift ($\delta$/ppm).

**Computational Method.** DFT calculations were carried out using Gaussian 16 rev. A. 03.[17] For all compounds, geometry and frequency optimizations have been performed in a continuum solvent. Hessian analysis indicates the absence of imaginary frequencies. Calculations were performed applying WB97XD as functionals, with the 6−311G+dp basis set. Acetone or THF environments were simulated with SMD as the continuum solvation model. Temperature was declared as an additional keyword.

**Synthesis of 1-Methyl-4-(prop-1-en-2-yl)-7-oxabicyclo[4.1.0]heptane (1).** In a two-neck round flask, (±) limonene (14.68 mmol, 2 g) was dissolved in dichloromethane (DCM), and the solution was stirred at −10 °C. m-CPBA (29.36 mmol, 5.1 g) was added dropwise to the solution through a dropping funnel (the temperature does not have to exceed −5 °C), and it was kept at −10 °C for 30 min, then 1 h at room temperature. After completion of the reaction, monitored by TLC, the mixture was quenched with a solution of NaOH 2 M (pH > 10) and extracted with DCM (3 × 30 mL); the combined organic layers were washed with a solution of $Na_2CO_3$, then dried over $Na_2SO_4$, filtered, and concentrated under reduced pressure. The crude was purified on silica gel (diethyl ether/light petroleum 1:9) to provide product **1** (8.9 mmol, 1.35 g, 60% yield) as a colorless oil. Rf: 0.4.

$^1$H NMR (400 MHz, Chloroform-d) $\delta$ 4.66 (q, $J$ = 1.4 Hz, 2H), 2.99 (d, $J$ = 5.4 Hz, 1H), 2.07−1.98 (m, 2H), 1.87 (ddt, $J$ = 12.3, 9.0, 6.2 Hz, 1H), 1.74−1.68 (m, 2H), 1.66 (d, $J$ = 1.2 Hz, 3H), 1.37 (tdt, $J$ = 8.2, 3.5, 1.4 Hz, 2H), 1.32 (s, 3H).

$^{13}$C NMR (101 MHz, Chloroform-d) $\delta$: 149.38, 109.22, 59.45, 57.69, 40.88, 30.89, 30.01, 24.47, 23.23, 20.36.

**Synthesis of 1-Methyl-2-(phenylselanyl)-4-(prop-1-en-2-yl)cyclohexan-1-ol (2).** In a two-neck round flask with inert atmosphere of $N_2$, diphenyl diselenide (9.56 mmol, 2.97 g) was dissolved in ethanol 98%; the mixture was cooled to 0 °C and $NaBH_4$ (19.13 mmol, 723.6 mg) was added portionwise. After the complete solubilization of the reagents, (±) limonene epoxide (7.97 mmol, 1.21 g) was added to the solution. The mixture was stirred for 12 h at room temperature. After completion of the reaction, monitored by TLC, ethanol was evaporated and the residue was washed with light petroleum, dried over $Na_2SO_4$, and the solvent was concentrated. The crude was purified by column chromatography (ethyl acetate/light petroleum 1:9) to obtain the product **2** (2.3 mmol, 711 mg, 29% yield) as a yellowish oil. Rf: 0.24.

$^1$H NMR (400 MHz, Chloroform-d) $\delta$ 7.61−7.53 (m, 2H), 7.29−7.25 (m, 3H), 4.73−4.67 (m, 2H), 3.43 (ddd, $J$ = 5.0, 3.6, 1.6 Hz, 1H), 2.36−2.28 (m, 1H), 2.20 (ddd, $J$ = 14.1, 10.5, 3.7 Hz, 1H), 1.90−1.78 (m, 2H), 1.67 (dd, $J$ = 1.4, 0.7 Hz, 3H), 1.66−1.59 (m, 3H), 1.41 (s, 3H).

$^{13}$C NMR (101 MHz, Chloroform-d) $\delta$: 148.84, 134.51, 130.58, 129.23, 127.60, 109.40, 72.69, 54.71, 39.64, 35.33, 33.80, 29.67, 26.34, 21.46.

Alternative procedure of the synthesis of **2** starting from **8**: in a two-neck round flask with inert atmosphere of $N_2$, diphenyl diselenide (9.56 mmol, 2.98 g) was dissolved in absolute ethanol. The mixture was cooled to 0 °C, and $NaBH_4$ (19.13 mmol, 723.6 mg) was added portionwise. After the complete solubilization of reagents, compound **8** (7.97 mmol, 1.86 g) was added to absolute ethanol. The mixture was stirred for 12 h at room temperature. After completion of the reaction, monitored by TLC, ethanol was evaporated, and the residue was washed with light petroleum, dried over $Na_2SO_4$, and the



https://doi.org/10.1021/acsomega.5c08636
ACS Omega 2026, 11, 5413−5420

solvent was evaporated. The crude was purified by chromatography (ethyl acetate/light petroleum 1:9) to obtain the product **2** (6.4 mmol, 1.98g, 80% yield) as a yellowish oil. Rf: 0.24.

After purification, we also characterized compound **6** obtained from this reaction.

$^1$H NMR (400 MHz, Chloroform-d) $\delta$ 7.61−7.57 (m, 2H), 7.38−7.27 (m, 3H), 4.74−4.67 (m, 2H), 3.88 (d, $J$ = 3.8 Hz, 1H), 2.37−2.20 (m, 3H), 1.83−1.78 (m, 2H), 1.74 (d, $J$ = 1.1 Hz, 3H), 1.67−1.56 (m, 2H), 1.37−1.33 (m, 3H).

$^{13}$C NMR (101 MHz, Chloroform-d) $\delta$: 149.49, 138.91, 134.77, 129.18, 129.18, 109.67, 73.00, 60.86, 38.50, 34.67, 33.98, 27.87, 26.39, 21.55.

**Synthesis of 2-Bromo-1-methyl-4-(prop-1-en-2-yl)-cyclohexan-1-ol (8).** (±) Limonene (14.7 mmol, 2 g) was dissolved in an acetone/water (8:2). The mixture was cooled to 0 °C, and NBS (17.65 mmol, 3.14 g) was added portionwise. The mixture was stirred for 1h at room temperature. After completion of the reaction, monitored by TLC, the solvent was evaporated, and the residue was washed with dichloromethane and water. The organic layer was dried over $Na_2SO_4$, and the solvent was concentrated. The crude was purified by chromatography (ethyl acetate/light petroleum 1,5:8,5) to obtain the product **8** (7.29 mmol, 1.7 g, 50% yield) as a colorless oil. Rf: 0.54.

$^1$H NMR (400 MHz, Chloroform-d) $\delta$ 4.78−4.73 (m, 2H), 4.20 (ddd, $J$ = 4.5, 3.5, 1.5 Hz, 1H), 2.50−2.41 (m, 1H), 2.27 (ddd, $J$ = 14.3, 10.9, 3.3 Hz, 1H), 2.05−1.93 (m, 2H), 1.76−1.72 (m, 3H), 1.66−1.61 (m, 2H), 1.60−1.55 (m, 1H), 1.43 (s, 3H).

$^{13}$C NMR (101 MHz, Chloroform-d) $\delta$: 148.88, 109.93, 72.19, 60.52, 38.80, 36.16, 33.62, 29.91, 26.50, 21.74.

**Synthesis of 2-Bromo-1-methyl-4-(prop-1-en-2-yl)-cyclohexyl Acetate (9).** Compound **8** (2.40 mmol, 0.56 g) was dissolved in 5 mL of acetonitrile (MeCN). Acetic anhydride (2.40 mmol, 245 mg, 0.227 mL) and $InBr_3$ (0.24 mmol, 0.085 g) were added to the solution. The mixture was stirred at room temperature for 15 min. After completion of the reaction, monitored by TLC, the solvent was evaporated, and the mixture was purified directly by chromatography (ethyl acetate/light petroleum 1:9) to obtain the product **9** (1.73 mmol, 0.48 g, 72% yield) as a colorless oil. Rf: 0.88.

$^1$H NMR (400 MHz, Chloroform-d) $\delta$ 4.88 (td, $J$ = 3.2, 1.9 Hz, 1H), 4.77−4.70 (m, 2H), 2.49 (ddd, $J$ = 11.6, 7.7, 4.0 Hz, 1H), 2.13 (dtd, $J$ = 14.4, 3.8, 1.9 Hz, 1H), 2.03 (s, 3H), 2.01−1.97 (m, 3H), 1.73 (ddd, $J$ = 1.3, 0.4 Hz, 3H), 1.66 (s, 3H), 1.65−1.43 (m, 2H).

$^{13}$C NMR (101 MHz, Chloroform-d) $\delta$: 170.11, 148.77, 109.38, 82.67, 55.59, 37.77, 35.40, 31.42, 26.12, 24.97, 22.35, 21.28.

**Synthesis of 2-Bromo-1-methoxy-1-methyl-4-(prop-1-en-2-yl)cyclohexane (10).** (±) Limonene (14.7 mmol, 2 g) was dissolved in a 50 mL solution of acetone/MeOH (8:2). The mixture was cooled to 0 °C, and NBS (17.65 mmol, 3.14 g) was added portionwise. The mixture was stirred for 1 h at room temperature. After completion of the reaction, monitored by TLC, the solvents were evaporated and the residue was extracted with dichloromethane and water. The organic layers were dried over $Na_2SO_4$, filtered, and the solvent was evaporated. The crude was purified by chromatography (ethyl acetate/light petroleum 1:9) to obtain the product **10** (4.85 mmol, 1.2 g, 33% yield) as a colorless oil. Rf: 0.76.

$^1$H NMR (400 MHz, Chloroform-d) $\delta$ 4.74−4.70 (m, 2H), 4.33 (td, $J$ = 3.1, 1.9 Hz, 1H), 3.21 (s, 3H), 2.49−2.41 (m, 1H), 2.20 (ddd, $J$ = 14.1, 11.9, 3.2 Hz, 1H), 1.96−1.77 (m, 3H), 1.73 (t, $J$ = 1.2 Hz, 3H), 1.69 (td, $J$ = 3.5, 2.0 Hz, 1H), 1.55−1.47 (m, 2H), 1.31 (s, 3H).

$^{13}$C NMR (101 MHz, Chloroform-d) $\delta$: 149.59, 109.51, 75.67, 58.76, 49.71, 38.53, 35.78, 30.37, 26.36, 23.87, 21.59.

**Synthesis of 1-Methyl-4-(prop-1-en-2-yl)cyclohex-2-en-1-ol (3).** Compound **2** (2.17 mmol, 0.67 g) was dissolved in 5 mL of DCM. The solution was cooled to 0 °C, and $H_2O_2$ (8.66 mmol, 0.98 mL) was added. The mixture was stirred at room temperature for 2h. After completion of the reaction, monitored by TLC, the solution was washed with water (2 × 25 mL) and extracted with 50 mL of DCM. The organic layers were dried over $Na_2SO_4$, filtered, and the solvent was concentrated. The crude was purified by chromatography (diethyl ether/light petroleum 2:8) to obtain product **3** (1.05 mmol, 0.16 g, 48% yield) as a yellowish oil. Rf: 0.20.

$^1$H NMR (400 MHz, Chloroform-d) $\delta$ 5.73−5.62 (m, 2H), 4.79−4.74 (m, 3H), 2.68−2.63 (m, 1H), 1.84−1.78 (m, 2H), 1.74 (dd, $J$ = 1.5, 0.8 Hz, 3H), 1.61−1.58 (m, 2H), 1.29 (s, 3H).

$^{13}$C NMR (101 MHz, Chloroform-d) $\delta$: 148.59, 134.35, 132.64, 111.06, 67.92, 43.86, 37.16, 29.85, 25.32, 21.34.

After purification, we also characterized compound **7** obtained from this reaction, even if not 100% pure, we can refer main peaks to compound **7**:

$^1$H NMR (400 MHz, Chloroform-d) $\delta$ 4.85 (t, $J$ = 1.8 Hz, 1H), 4.77 (td, $J$ = 2.0, 0.6 Hz, 1H), 4.72−4.69 (m, 2H), 4.37 (t, $J$ = 3.3 Hz, 1H), 2.58−2.43 (m, 2H), 2.21 (dt, $J$ = 13.6, 3.7 Hz, 1H), 1.99 (dtd, $J$ = 13.7, 3.5, 2.3 Hz, 2H), 1.85 (dddd, $J$ = 11.6, 7.3, 2.8, 1.8 Hz, 2H), 1.72 (t, $J$ = 1.1 Hz, 3H).

$^{13}$C NMR (101 MHz, Chloroform-d) $\delta$: 149.97, 149.57, 110.00, 109.04, 72.56, 39.16, 38.27, 32.72, 30.08, 21.14.

**Synthesis of 5′-Methyl-4-pentyl-2′-(prop-1-en-2-yl)-1′,2′,3′,4′-tetrahydro-[1,1′-biphenyl]-2,6-diol (±)-CBD.** Olivetol (5.16 mmol, 0.93 g) was dissolved in 10 mL of dry dichloromethane under nitrogen and was added via a syringe to a nitrogen-flushed flask containing $MgSO_4$ (5.65 mmol, 680 mg). The mixture was cooled to 0 °C, and $BF_3$-diethyl etherate (0.25 mmol, 35 mg, 0.03 mL) was added to the mixture. Compound **3** (4.12 mmol, 0.63 g) was dissolved in 5 mL of dry DCM and cooled to 0 °C. The cold solution was then added dropwise to the cold mixture. The reaction was stirred at 0 °C for 1.5 h and then at room temperature for 24 h. After reaction completion, monitored by TLC, the reaction was quenched by the addition of 30 mL of sat. $NaHCO_3$, and the layers were separated by a separatory funnel. The water phase was then extracted three times with 20 mL each of DCM. The combined organic phases were washed with brine, dried over $Na_2SO_4$, filtered, and evaporated. The crude product was purified by chromatography (ethyl acetate/light petroleum 3:7) to obtain the product **racemic CBD** (1.28 mmol, 0.40 g, 30% yield) as a brownish oil. Rf: 0.75.

The final product was then separated by chiral chromatography, and we obtained the NMR spectra of (−)-CBD and (+)-CBD.

**(1′S,2′S)-5′-Methyl-4-pentyl-2′-(prop-1-en-2-yl)-1′,2′,3′,4′-tetrahydro-[1,1′-biphenyl]-2,6-diol (+)-CBD.** $^1$H NMR (500 MHz, Methanol-d4) $\delta$ 6.08 (s, 2H), 5.29 (dt, $J$ = 2.3, 1.2 Hz, 1H), 4.47 (d, $J$ = 2.6 Hz, 1H), 4.43 (dq, $J$ = 2.8, 1.5 Hz, 1H), 3.93 (ddq, $J$ = 10.8, 4.6, 2.3 Hz, 1H), 2.91 (td, $J$ = 10.3, 5.3 Hz, 1H), 2.41−2.35 (m, 2H), 2.25−2.16 (m, 1H),



https://doi.org/10.1021/acsomega.5c08636
ACS Omega 2026, 11, 5413−5420

2.04−1.97 (m, 1H), 1.74 (td, $J$ = 10.9, 9.8, 5.7 Hz, 2H), 1.68 (dt, $J$ = 2.5, 1.2 Hz, 3H), 1.64 (t, $J$ = 1.1 Hz, 3H), 1.61−1.51 (m, 2H), 1.38−1.28 (m, 4H), 0.90 (t, $J$ = 7.1 Hz, 3H).

$^{13}$C NMR (126 MHz, MeOD) $\delta$: 157.50, 157.47, 150.38, 142.68, 134.13, 127.36, 115.98, 110.48, 108.27, 46.35, 37.48, 36.60, 32.66, 32.04, 31.71, 30.77, 23.70, 23.60, 19.50, 14.40.

**(1′R,2′R)-5′-Methyl-4-pentyl-2′-(prop-1-en-2-yl)-1′,2′,3′,4′-tetrahydro-[1,1′-biphenyl]-2,6-diol (−)-CBD.** $^1$H NMR (500 MHz, Methanol-d4) $\delta$ 6.09 (s, 2H), 5.30 (d, $J$ = 2.7 Hz, 1H), 4.48 (d, $J$ = 2.6 Hz, 1H), 4.44 (dd, $J$ = 2.7, 1.4 Hz, 1H), 3.93 (ddt, $J$ = 10.7, 4.4, 2.3 Hz, 1H), 2.92 (td, $J$ = 10.3, 5.3 Hz, 1H), 2.39 (t, $J$ = 7.7 Hz, 2H), 2.25−2.17 (m, 1H), 2.07−1.98 (m, 1H), 1.76 (dd, $J$ = 9.1, 4.0 Hz, 2H), 1.71−1.68 (m, 3H), 1.65 (d, $J$ = 1.3 Hz, 3H), 1.56 (p, $J$ = 7.5 Hz, 2H), 1.39−1.27 (m, 5H), 0.91 (t, $J$ = 7.0 Hz, 3H).

$^{13}$C NMR (126 MHz, MeOD) $\delta$ 156.03, 148.97, 141.28, 132.73, 125.95, 114.58, 109.08, 106.91, 44.94, 36.08, 35.20, 31.25, 30.63, 30.31, 29.36, 22.30, 22.20, 18.09, 13.00.

## ■ ASSOCIATED CONTENT

### Supporting Information

The Supporting Information is available free of charge at https://pubs.acs.org/doi/10.1021/acsomega.5c08636.

DFT studies (Tables S1−S3) (Figure S1); Cartesian coordinates, chiral HPLC (Figures S2−S5), optimization data (Table S4), and $^1$H NMR, $^{13}$C{$^1$H} NMR, $^1$H−$^1$H COSY, and HSQC (Figures S6−S27) (PDF)

## ■ AUTHOR INFORMATION


### Corresponding Author

**Anna Fantinati** − *Department of Environmental and Prevention Sciences, University of Ferrara, 44121 Ferrara, Italy;* orcid.org/0000-0003-0437-5670; Email: anna.fantinati@unife.it

### Authors

**Michael Bergami** − *Department of Environmental and Prevention Sciences, University of Ferrara, 44121 Ferrara, Italy*

**Claudio Trapella** − *Illuminati Department of Chemical, Pharmaceutical and Agricultural Sciences University of Ferrara, 44121 Ferrara, Italy;* orcid.org/0000-0002-6666-143X

**Greta Compagnin** − *Illuminati Department of Chemical, Pharmaceutical and Agricultural Sciences University of Ferrara, 44121 Ferrara, Italy*

**Simona Felletti** − *Department of Environmental and Prevention Sciences, University of Ferrara, 44121 Ferrara, Italy;* orcid.org/0000-0002-4192-2074

**Martina Catani** − *Illuminati Department of Chemical, Pharmaceutical and Agricultural Sciences University of Ferrara, 44121 Ferrara, Italy;* orcid.org/0000-0003-4217-8766

**Silvia Pezzola** − *Department of Chemical Science and Technologies, University of Rome "Tor Vergata", 00133 Rome, Italy*

**Federica Sabuzi** − *Department of Chemical Science and Technologies, University of Rome "Tor Vergata", 00133 Rome, Italy;* orcid.org/0000-0002-3757-0598

**Pierluca Galloni** − *Department of Chemical Science and Technologies, University of Rome "Tor Vergata", 00133 Rome, Italy;* orcid.org/0000-0002-0941-1354

**Paolo Marchetti** − *Illuminati Department of Chemical, Pharmaceutical and Agricultural Sciences University of Ferrara, 44121 Ferrara, Italy*

**Virginia Cristofori** − *Illuminati Department of Chemical, Pharmaceutical and Agricultural Sciences University of Ferrara, 44121 Ferrara, Italy;* orcid.org/0000-0002-6837-6042

**Davide Illuminati** − *Illuminati Department of Chemical, Pharmaceutical and Agricultural Sciences University of Ferrara, 44121 Ferrara, Italy;* orcid.org/0000-0002-0321-1941

Complete contact information is available at: https://pubs.acs.org/10.1021/acsomega.5c08636


### Notes

The authors declare no competing financial interest.

## ■ ACKNOWLEDGMENTS

The research was funded by National Recovery and Resilience Plan (NRRP), Mission 04 Component 2 Investment 1.5—NextGenerationEU, Call for tender n. 3277 dated 30 December 2021. Award Number: 0001052 dated 23 June 2022 (C.T.) and by the 2023 CCIAA Grant (Bando 2023 CCIAA), awarded to Anna Fantinati, cofunded by the University of Ferrara. CUP: F73C24001330005. G.C., S.F., and M.C. would like to thank the Italian University and Scientific Research Ministry (grant P2022PTYWP), title: "Design of highpRofit fostEring bioActive coMpounds through integral valorization of seaWEEDs infesting the MEditerranean sea (DreamWEEDme). C.T., P.M., A.F., and V.C. thank University of Ferrara FAR 2024. S.P., F.S., and P.G. thank Grant MUR Dipartimento di Eccellenza 2023-27 "XCHEM-project"eXpanding CHEMistry: implementing excellence in research and teaching."

## ■ REFERENCES

(1) Crocq, M.-A. History of cannabis and the endocannabinoid system. *Dialogues Clin. Neurosci.* **2020**, *22*, 223−228.

(2) Fasinu, P. S.; Phillips, S.; Elsohly, M. A.; Walker, L. A. Current Status and prospects for cannabidiol preparations as new therapeutic agents. *Pharmacotherapy* **2016**, *36*, 781−796.

(3) Singh, K.; Bhushan, B.; Chanchal, D. K.; Sharma, S. K.; Rani, K.; Yadav, M. K.; Porwal, P.; Kumar, S.; Sharma, A.; Virmani, T.; Kumar, G.; Noman, Al. A. Emerging Therapeutic Potential of Cannabidiol (CBD) in Neurological Disorders: A Comprehensive Review. *Behav. Neurol.* **2023**, *2023*, No. 8825358.

(4) Cioffi, C. L.; Lotsaris, I.; Cantwell, R. P.; Pati, T. K.; Suleria, K.; Mahesh, G.; Singh, S.; Peiser-Oliver, J.; Mohammadi, S.; Vandenberg, R. J. Current Nonopioid Small Molecule Approaches Toward the Treatment of Neuropathic Pain. *J. Med. Chem.* **2025**, *68* (17), 18064−18098.

(5) Wood, J. S.; Gordon, W. H.; Morgan, J. B.; Williamson, R. T. Cannabicitran: Its unexpected racemic nature and potential origins. *Chirality* **2023**, *35*, 540−548.

(6) Fride, E.; Feigin, C.; Ponde, D. E.; Breuer, A.; Hanus, L.; Arshavsky, N.; Mechoulam, R. (+)-Cannabidiol analogues which bind cannabinoid receptors but exert peripheral activity only. *Eur. J. Pharmacol.* **2004**, *506*, 179−188.

(7) Leite, J. R.; Carlini, E. A.; Lander, N.; Mechoulam, R. Anticonvulsant effect of (−) and (+) isomers of CBD and their dimethyl heptyl homologs. *Pharmacology* **1982**, *24*, 141−146.

(8) Wang, X.; Zhang, H.; Liu, Y.; Xu, Y.; Yang, B.; Li, H.; Chen, L. An overview on synthetic and biological activities of cannabidiol (CBD) and its derivatives. *Bioorg. Chem.* **2023**, *140*, No. 106810.
(9) Mori, K. Synthesis of (1*S*,4*R*)-4-isopropyl-1-methyl-2-cyclohexen-1-ol, the aggregation pheromone of the ambrosia beetle *Platypus quercivorus*, its racemate, (1*R*,4*R*)- and (1*S*,4*S*)-isomers. *Tetrahedron: Asymmetry* **2006**, *17*, 2133−2142.
(10) Lavi, Y.; Kogan, N. M.; Topping, L. M.; Liu, C.; McCann, F. E.; Williams, R. O.; Breuer, A.; Yekhtin, Z.; Ezra, A. F.; Gallily, R.; Feldmann, M.; Mechoulam, R. Novel Synthesis of C-Methylated Phytocannabinoids Bearing Anti-inflammatory Properties. *J. Med. Chem.* **2023**, *66*, 5536−5549.
(11) Chai, J.-D.; Head-Gordon, M. Long-range corrected hybrid density functionals with damped atom-atom dispersion corrections. *Phys. Chem. Chem. Phys.* **2008**, *10*, 6615−6620.
(12) Kosar, N.; Ayub, N.; Gilani, M. A.; Muhammad, S.; Mahmood, T. Benchmark Density Functional Theory Approach for the Calculation of Bond Dissociation Energies of the M−O2 Bond: A Key Step in Water Splitting Reactions. *ACS Omega* **2022**, *7*, 20800−20808.
(13) Lee, D.; Yamauchi, K.; Sakai, K. Water-Induced Switching in Selectivity and Steric Control of Activity in Photochemical CO2 Reduction Catalyzed by RhCp*(bpy). *J. Am. Chem. Soc.* **2024**, *146*, 31597−31611.
(14) Pezzola, S.; Venanzi, M.; Galloni, P.; Conte, V.; Sabuzi, F. Towards the "Eldorado" of pKa Determination: A Reliable and Rapid DFT Model. *Molecules* **2024**, *29*, No. 1255.
(15) Foresman, J. B.; Frisch, Æ. *Exploring Chemistry with Electronic Structure Methods*; Gaussian, Inc: Wallingford, CT, 2015.
(16) Curtiss, L. A.; McGrath, M. P.; Blaudeau, J.-P. E.; Davis, N. E.; Binning, R. C.; Radom, J. L. Extension of Gaussian-2 theory to molecules containing third-row atoms Ga−Kr. *J. Chem. Phys.* **1995**, *103*, 6104−6113.
(17) Frisch, M. J.; Trucks, G. W.; Schlegel, H. B.; Scuseria, G. E.; Robb, M. A.; Cheeseman, J. R.; Scalmani, G.; Barone, V.; Petersson, G. A.; Nakatsuji, H.; Li, X.; Caricato, M.; Marenich, A. V.; Bloino, J.; Janesko, B. G.; Gomperts, R.; Mennucci, B.; Hratchian, H. P.; Ortiz, J. V.; Izmaylov, A. F.; Sonnenberg, J. L.; Williams-Young, D.; Ding, F.; Lipparini, F.; Egidi, F.; Goings, J.; Peng, B.; Petrone, A.; Henderson, T.; Ranasinghe, D.; Zakrzewski, V. G.; Gao, J.; Rega, N.; Zheng, G.; Liang, W.; Hada, M.; Ehara, M.; Toyota, K.; Fukuda, R.; Hasegawa, J.; Ishida, M.; Honda, Y.; Kitao, O.; Nakai, H.; Vreven, T.; Throssell, K.; Montgomery, J. A., Jr; Peralta, J. E.; Ogliaro, F.; Bearpark, M. J.; Heyd, J. J.; Brothers, E. N.; Kudin, K. N.; Staroverov, V. N.; Keith, T. A.; Kobayashi, R.; Normand, J.; Raghavachari, K.; Rendell, A. P.; Burant, J. C.; Iyengar, S. S.; Tomasi, J.; Cossi, M.; Millam, J. M.; Klene, M.; Adamo, C.; Cammi, R.; Ochterski, J. W.; Martin, R. L.; Morokuma, K.; Farkas, O.; Foresman, J. B.; Fox, D. J. *Gaussian 16*; Gaussian; Inc.: Wallingford CT, 2016.




https://doi.org/10.1021/acsomega.5c08636
*ACS Omega* 2026, 11, 5413−5420